DEFORMATION OF THE BANDED TERRAIN OF HELLAS PLANITIA, MARS. C. W. Cook[1], S. Byrne[1], and M. M. Sori[2], [1]Lunar and Planetary Laboratory, University of Arizona, Tucson, AZ 85721 (clairec@lpl.arizona.edu), [2]Purdue University

Introduction: The extent of past glaciation on Mars is an important unknown in determining its water inventory and climate history. Understanding the origin of the banded terrain in Hellas basin could shed light on this aspect of martian history. Banded terrain is a surface morphology, ~1.9–3.7 Gyr old, composed of bands with linear, lobate, and concentric forms found primarily in northwest Hellas basin (Fig. 1 a–c) [1, 2]. Linear bands are typically ~5 km long, 300 m wide, and 10 m in relief [2]. In some locations, banded terrain superposes honeycomb terrain, which is made up of adjacent ~10 km wide depressions [3] (Fig. 1 d).

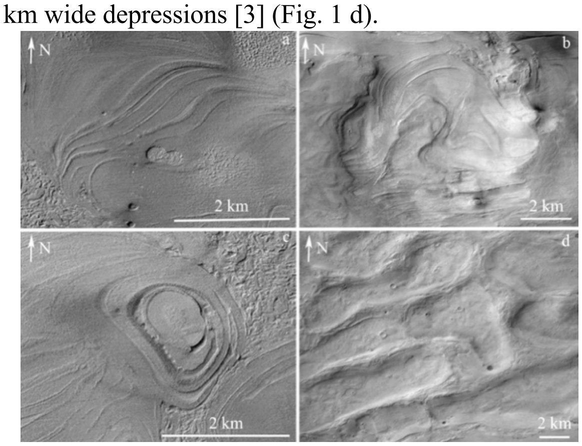

Figure 1: Examples of a) linear banded terrain, b) lobate banded terrain, c) concentric banded terrain, and d) honeycomb terrain. CTX image D21_035353_1431.

Bands starting at topographic highs, and polygons that signify the presence of ground ice, led Diot et. al. [2, 4] to suggest banded terrain was due to gravity driven viscous flow of a thin ice-rich layer. However, more comprehensive topography measurements by Bernhardt et al. [1] suggested that band orientation does not always correlate with local slopes, making gravity-driven flow unlikely. They suggest small-scale stresses resulting from a thick ice sheet superposing the honeycomb terrain deformed subglacial sediment.

The latter interpretation is supported by observations and modeling of some terrestrial subglacial landforms. Ribbed bedforms, which are curvilinear ridges mostly transverse to ice-flow direction, are found over large areas of past ice sheets [5]. They exist at a large range of scales, including some at scales similar to banded terrain of ~ 3 km long, ~700 m wide, and ~15 m amplitude [5]. Models of the coupled flow of ice and subglacial sediment have shown that a wave-like instability can lead to the formation of ribbed bedforms at various scales [6, 7].

Here, we perform quantitative modeling to test the hypothesis that banded terrain may be formed by subglacial till deformation.

Methods: We use the finite element modeling software COMSOL to simulate banded terrain formation via deformation of ice and subglacial till. Subglacial till is modeled over a small area with a prescribed surface velocity representing the basal velocity of a larger ice sheet. This velocity and other parameters are varied to determine which, if any, may lead to till deformation on the scale of banded terrain. A larger scale, lower resolution model of an ice sheet in the Hellas basin will be used to determine ice sheet properties and thermal parameters that lead to the basal velocity required for till deformation.

Till rheology is modeled using a viscous flow law (as in [8]) of the form: $\dot{\varepsilon} = B^{-m}{\tau_E}^{m-1}\tau$ where $\dot{\varepsilon}$ is the strain rate, B is the hardness factor, τ_E is the effective stress ($\sqrt{J_2}$, where J_2 is the second invariant of the deviatoric stress), τ is the deviatoric stress, and *m* is the stress exponent. Till has been described as having a moderately nonlinear viscous behavior in some studies, corresponding to a small value of the stress exponent (~3), but as nearly plastic in other studies, corresponding to a large value of the stress exponent (~40). We will vary the hardness factor and stress exponent parameters, as well as the till thickness and velocity at the top surface of the till. The basal geometry is based on a power-law noise surface (Fig. 2, with spectral exponent 1.8), while the initial top surface of the till is flat. The basal velocity is set to zero, and the side boundary conditions are periodic (to simulate that the till extends beyond the modeled domain).

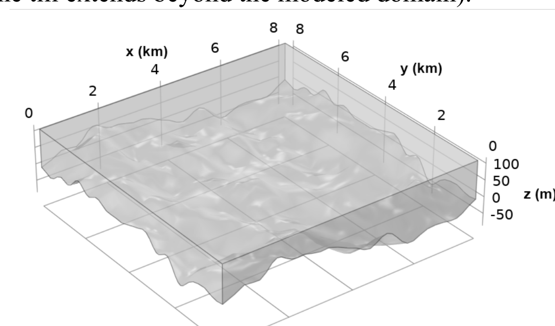

Figure 2: Geometry for the subglacial till model using a power-law noise surface. The minimum till thickness is 30 m. Vertical exaggeration is 10.

Ice rheology is modeled using a similar viscous flow law: $\dot{\varepsilon} = Ae^{-2n\varphi}e^{-Q/RT}{\tau_E}^{n-1}\tau d^{-p}$ where A is a material parameter, *n* is the stress exponent, φ is the dust volume fraction, Q is activation energy, R is the gas constant, T is temperature, τ_E is the effective stress, τ is the deviatoric stress, d is the grain size, and p is the grain size exponent [9]. We include dislocation creep, grain boundary sliding, and basal slip deformation mechanisms, with different parameters for these three modes. Ice temperatures will be set to the annual-average surface temperature and increase with depth at a rate set by the martian geotherm. We will vary the ice thickness, surface temperature, and geothermal heat flux. Given the early time period for banded terrain formation, we will consider a wide range of possible surface temperatures and heat flux. We will include subglacial water for high values of these parameters (e.g., surface temperature over 260 K and geothermal heat flux over 50 mW/m^2), for which melting can occur at the base of the ice.

Results: In our model of a one km thick, dome-shaped, isothermal ice sheet centered in Hellas basin, velocity is highest in the northwest portion of Hellas, in the trough where banded terrain is located, which could be related to why banded terrain is found primarily in this area of the basin. Fig. 3 shows the horizontal magnitude of surface velocity from this model.

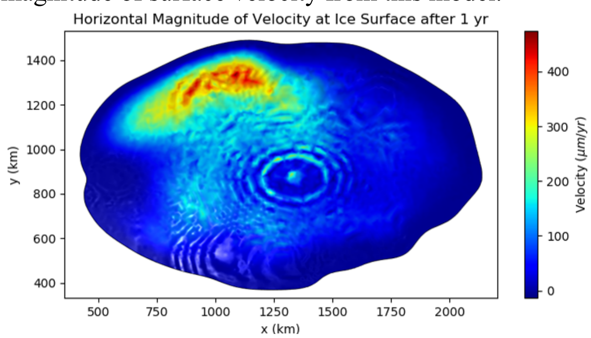

Figure 3: Top-down view of the surface of an ice sheet within Hellas basin, showing the horizontal magnitude of surface velocity after 1 yr. The maximum ice thickness is 1 km, and the temperature is a constant 200 K.

In this model, the basal velocity is set to zero, because the till layer, or other mechanisms of basal sliding are not included. A till layer will be added to find accurate basal velocities in an iterative process with the till model described below. The large-scale ice flow model will then be used to find ice sheet parameters that give the basal velocity needed for till deformation on the scale of banded terrain.

In our till model, for some values of surface velocity, ridges form in the surface of the till. For example, Fig. 4 shows the vertical displacement at the surface of the till for a model run for 100 years, with a velocity at the top of the till of 0.1 m/yr (in the positive y direction), with till parameters of m=3 and B=3.5×10^7 Pa s$^{1/3}$ (corresponding to till that is moderately nonlinear and that is less viscous than ice). Over 100 years, ridges form mostly transverse to the flow direction with amplitudes of ~0.5 m and lengths of several kilometers. Models with a coarser mesh run for 1000 years show vertical displacement of tens of meters. The locations of these ridges are constant over time, but the features grow in relief. After 1000 years, they still have not reached a steady-state amplitude.

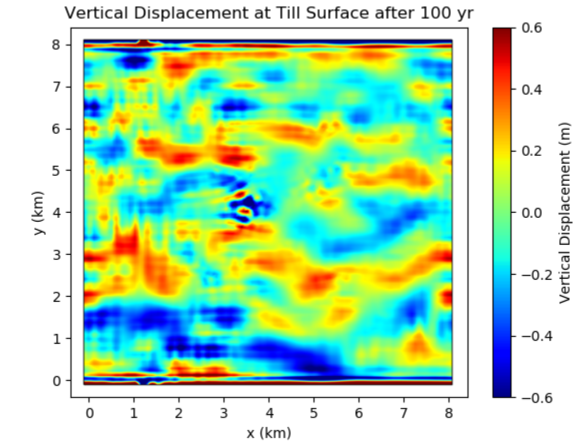

Figure 4: Top-down view of the surface of the till, showing the vertical component of displacement (in m) after 100 years.

For a smaller ice-sheet velocity at the top of the till, such as 10^{-3} m/yr, there is less deformation over a given period of time. Because of the non-Newtonian rheology, deformation rates are non-linearly dependent on ice velocity with 100× faster velocities yielding less than 100× more deformation.

The hypothesis that subglacial till deformation could have formed banded terrain is supported by the maximum velocities in a Hellas ice sheet occurring in the trough where banded terrain is located. However, more work is needed to include a till layer in this model to find realistic basal velocities for a range of conditions. This hypothesis is also supported by the 0.5 m scale deformation observed in our till model over 100 years. At this rate, ridges with the 10 m relief of banded terrain could form in ~2000 years. However, more work is needed to ensure these results are robust by using finer meshes and basal topography from CTX DTMs.

References: [1] Bernhardt H. et. al. (2019) *Icarus, 321*, 171-188. [2] Diot X. et. al. (2014) *Planetary & Space Science, 101*, 118-134. [3] Bernhardt H. et. al. (2016) *JGR, 121*, 714-738. [4] Diot X. et. al. (2015) *JGR, 120*, 2258-2276. [5] Stokes C. R. et al. (2016) *J. Glaciology 62*, 696-713. [6] Dunlop P. et al. (2008) *JGR, 113*, F03005. [7] Fowler A. C and Chapwanya M. (2014) *Proc. R. Soc. A, 470*, 20140185. [8] Leysinger-Vieli G.J-M.C. and Gudmundsson G. H. (2010) *Cryosphere, 4*, 359-372. [9] Goldsby D. L and Kohlstedt D. L. (2001) *JGR, 106*, 11017-11030.